


# Multifaceted Brain Networks Reconfiguration in Disorders of Consciousness Uncovered by Co-Activation Patterns

Carol Di Perri <sup>1,2,\*</sup> Enrico Amico,<sup>1,3,4</sup> Lizette Heine,<sup>1</sup> Jitka Annen,<sup>1</sup> Charlotte Martial,<sup>1</sup> Stephen K. Larroque,<sup>1</sup> Andrea Soddu,<sup>5</sup> Daniele Marinazzo,<sup>3</sup> and Steven Laureys<sup>1</sup>

<sup>1</sup>Coma Science Group, GIGA Research Center, University of Liège, Liège, Belgium

<sup>2</sup>Centre for Clinical Brain Sciences, Centre for Dementia Prevention, UK Dementia Research Institute, University of Edinburgh, Edinburgh, United Kingdom

<sup>3</sup>Department of Data-analysis, University of Ghent, Ghent B9000, Belgium

<sup>4</sup>School of Industrial Engineering, Purdue University, West Lafayette, Indiana

<sup>5</sup>Brain and Mind Institute, Physics & Astronomy Department, Western University, London, Ontario, Canada



**Abstract:** *Introduction:* Given that recent research has shown that functional connectivity is not a static phenomenon, we aim to investigate the dynamic properties of the default mode network's (DMN) connectivity in patients with disorders of consciousness. *Methods:* Resting-state fMRI volumes of a convenience sample of 17 patients in unresponsive wakefulness syndrome (UWS) and controls were reduced to a spatiotemporal point process by selecting critical time points in the posterior cingulate cortex (PCC). Spatial clustering was performed on the extracted PCC time frames to obtain 8 different co-activation patterns (CAPs). We investigated spatial connectivity patterns positively and negatively correlated with PCC using both CAPs and standard stationary method. We calculated CAPs occurrences and the total number of frames. *Results:* Compared to controls, patients showed (i) decreased within-network positive correlations and between-network negative correlations, (ii) emergence of “pathological” within-network negative correlations and between-network positive correlations (better defined with CAPs), and (iii) “pathological” increases in within-network positive correlations and between-network negative correlations (only detectable using CAPs). Patients showed decreased occurrence of DMN-like CAPs (1–2) compared to controls. No between-group differences were observed in the total number of frames. *Conclusion:* CAPs reveal at a more fine-grained level the multifaceted spatial connectivity reconfiguration following the DMN disruption in UWS patients, which is more complex than previously thought and suggests alternative anatomical substrates for consciousness. BOLD fluctuations do

Additional Supporting Information may be found in the online version of this article.

Contract grant sponsors: Belgian Funds for Scientific Research (FRS), European Commission, Luminous, Center-TBI, Human Brain Project, James McDonnell Foundation, European Space Agency, Belspo, “Fondazione Europea di Ricerca Biomedica,” BIAL Foundation, Wallonia-Brussels Federation Concerted Research Action, and Mind Science Foundation.

Carol Di Perri and Enrico Amico contributed equally to this work.

\*Correspondence to: Carol Di Perri, MD, PhD and Steven Laureys, MD, PhD; Coma Science Group, GIGA (ULg) B34, Quartier Hôpital, Avenue de l'Hôpital, 11, 4000 Sart-Tilman, Belgium. E-mails: [diperric@gmail.com](mailto:diperric@gmail.com) and [steven.laureys@ulg.ac.be](mailto:steven.laureys@ulg.ac.be)

Received for publication 12 April 2017; Revised 11 August 2017; Accepted 18 September 2017.

DOI: 10.1002/hbm.23826

Published online 00 Month 2017 in Wiley Online Library ([wileyonlinelibrary.com](http://wileyonlinelibrary.com)).

not seem to differ between patients and controls, suggesting that BOLD response represents an intrinsic feature of the signal, and therefore that spatial configuration is more important for consciousness than BOLD activation itself. *Hum Brain Mapp* 00:000–000, 2017. © 2017 Wiley Periodicals, Inc.

**Key words:** unresponsive wakefulness syndrome; co-activation patterns; pathological hyperconnectivity; dynamic network interactions

## INTRODUCTION

Disorders of consciousness represent a spectrum of clinical conditions involving profound disruption in the level of consciousness due to important brain damage [Giacino et al., 2014]. Patients in vegetative state, now also called unresponsive wakefulness syndrome (UWS) [Laureys et al., 2010], are awake but show no signs of awareness of themselves or their environment [Di Perri et al., 2014].

Significant discoveries regarding the neural correlates underlying these states of unconsciousness have recently been made, partly due to the progress of functional neuroimaging techniques such as resting-state functional MRI (fMRI) [Di Perri et al., 2014].

It has been shown that awareness is not unequivocally related to a specific anatomical brain region, but rather to the activity and complex functional interconnections within a widespread fronto-parietal network encompassing associative cortices and between this network and the thalamus [Laureys, 2005]. This network has been subdivided into two networks related on one hand to the perception of one's self and on the other hand to the perception of the external environment: the internal and the external awareness networks respectively [Vanhaudenhuyse et al., 2011]. The internal awareness network, also called default mode network (DMN), involves midline regions, such as anterior cingulate cortex and precuneus/posterior cingulate cortex and temporo-parietal junctions and the hippocampi [Vanhaudenhuyse et al., 2011]. The external awareness network, also known as task positive network, encompasses mainly lateral frontoparietal hemispheric regions [Fox et al., 2005].

Studies using resting-state fMRI have shown that the DMN and the external awareness network exhibit spontaneous competing anticorrelated activity (i.e., between-network negative correlations or anticorrelations) [Fox et al., 2005; Vanhaudenhuyse et al., 2011]. The dynamic interaction between these two networks is robust and reliable in healthy controls [Damoiseaux et al., 2006], while impaired in patients with disorders of consciousness [Di Perri et al., 2016]. At present, the global hallmark of impaired consciousness following a severe brain injury appears to be a complex dysfunctional connectivity pattern. Indeed, loss of both within-network positive correlations (i.e., positive correlations in the DMN) and between-network negative correlations (i.e., negative correlations between the DMN and the external awareness network), and emergence of “pathological” between-network positive

correlations (i.e., positive correlations between the DMN and the external awareness network) appear to be all involved [Di Perri et al., 2016]. We should however keep in mind that a dynamic reconfiguration of DMN interactions with other networks has been also observed to a certain extent in healthy controls [Karahanoglu and Van De Ville, 2015; Vatansever et al., 2015], suggesting that positive correlations between these two networks are not necessarily pathological, but an altered balance might indeed generate pathology.

Most resting-state fMRI studies have implicitly assumed that the interaction of signal between distinct brain regions is constant during recording periods. Recent research has however shown that functional connectivity of the brain is not a static phenomenon: instead, it exhibits spontaneous fluctuation over time [Allen et al., 2014; Chang and Glover, 2010; Hutchison et al., 2013]. For example, magnetoencephalography analyses—and local field potentials—have shown a time-varying relation between the main nodes of the DMN and the external awareness network, ranging from positive to negative values [Chang and Glover, 2010; de Pasquale et al., 2010; Hutchison et al., 2013]. Similarly, temporal variability in the BOLD signals has also been examined over resting-state scans of healthy volunteers, confirming the dynamic nature of functional connectivity [Chang and Glover, 2010; Hutchison et al., 2013; Kang et al., 2011; Kiviniemi et al., 2011; Laumann et al., 2016]. Hence, the focus of research on resting-state fMRI has recently shifted from the analysis of functional connectivity averaged over the duration of scanning sessions to the analysis of changes of functional connectivity within sessions [Karahanoglu and Van De Ville, 2015]. As a consequence, different methodologies have been adopted. The most straightforward approach, using sliding windows, appears to be problematic, particularly as far as fMRI data are concerned. Indeed, this analysis is often limited to a few brain regions of interest and it is hampered by the confounding contribution of non-neurogenic signals such as motion, instrumental drift, and thermal noise, which is difficult to distinguish from the signals of interest, especially when using shorter sliding time windows. Furthermore, results are strongly dependent on window length, whose optimal length to now remains somewhat ambiguous [Chang and Glover, 2010; Shakil et al., 2016]. For these reasons, alternative approaches have been proposed [Hindriks et al., 2016; Leonardi and Van De Ville, 2015; Lindquist et al., 2014]. Spatial clustering of BOLD co-activation over only a few critical time points constitutes a valid and robust alternative, which is able to

capture the patterns variety of dynamical brain states [Liu et al., 2013]. According to the latter approach inspired by point process analysis [Tagliazucchi et al., 2012], much of the information obtained in a resting-state acquisition can be reduced to a number of critical time-points, also called frames, where the seed regions' signal exceeds a threshold. By decomposing the BOLD signal into posterior cingulate cortex (PCC) co-activation patterns (CAPs) at these critical time points, more fine-grained DMN-related functional connectivity information have been detected when compared to standard seed-based resting-state fMRI analysis in conscious subjects and propofol-mediated states of consciousness [Amico et al., 2014; Liu et al., 2013]. For example, as above mentioned, two different DMN related CAPs have been observed to differently interact with the external awareness network in awake controls [Karahanoglu and Van De Ville, 2015]. Furthermore, decreased activity in motor and visual areas—not detectable using standard functional connectivity methods—has been observed in propofol-induced unconsciousness states [Amico et al., 2014].

In this cross-sectional study, we apply this methodology to brain-injured unconscious patients (unresponsive wakefulness syndrome, UWS). We aim to obtain additional spatiotemporal networks' information valuable for a better understanding of the dysfunctional connectivity patterns underlying pathological states of consciousness. As we recently demonstrated the importance of negative correlations between the DMN and the external awareness network for cognitive functions necessary to recover from disorders of consciousness [Di Perri et al., 2016], we further decompose the BOLD signal into negative CAPs. By doing so, we aim to further investigate the between-networks' interactions in healthy and diseased subjects. Finally, we calculate the temporal occurrences of CAPs and the total number of frames in each group to investigate CAPs distribution and BOLD fluctuations, respectively.

## MATERIALS AND METHODS

### Subjects

Two groups were included: patients in UWS and healthy controls.

Unresponsive patients were behaviorally assessed with the Coma Recovery Scale Revised (CRS-R) [Giacino et al., 2004] and diagnosed as UWS (see Supporting Information 1 for diagnostic criteria). Exclusion criteria were (i) neuro-imaging examination in an acute state, that is, <28 days from brain insult, (ii) sedation or anesthesia during scanning, (iii) large focal brain damage, that is, >1/3 of one hemisphere, as stated by a certified neuroradiologist, (iv) motion parameters >3 mm in translation and 3° in rotation, (v) suboptimal segmentation and spatial normalization as stated by a certified neuroradiologist, and (vi) psychiatric or neurological history.

The study was approved by the Ethics Committee of the Medical School of the University of Liège, written informed consent to participate in the study was obtained from the healthy subjects and from the legal surrogates of the patients.

### Data Acquisition

Three hundred T2\*-weighted functional magnetic resonance imaging (fMRI) resting-state volumes (Echo Planar Imaging sequence: 32 slices, repetition time = 2,000 ms, echo time = 30 ms, field of view =  $192 \times 192 \text{ mm}^2$ , flip angle =  $78^\circ$ , voxel size =  $3 \times 3 \times 3 \text{ mm}^3$ ) and one high-resolution T1-weighted image (T1-weighted 3D gradient echo images using 120 slices, repetition time = 2,300 ms, echo time = 2.47 ms, voxel size =  $1 \times 1 \times 1.2 \text{ mm}^3$ , flip angle =  $9^\circ$ , field of view =  $256 \times 256 \text{ mm}^2$ ) were acquired on a 3 T scanner (Siemens Trio Tim, Munich, Germany).

### Data Preprocessing

fMRI resting-state data preprocessing was performed using SPM8 (Statistical Parametric Mapping 8, [www.fil.ion.ucl.ac.uk/spm](http://www.fil.ion.ucl.ac.uk/spm)). Preprocessing steps included slice-time correction, realignment, co-registration of functional on structural data, regression of 6 motion regressors (3 translations [ $x, y, z$ ] and 3 rotations [pitch, yaw, and roll]) and 3 tissue regressors (mean signal of whole-brain, white matter (WM), and cerebrospinal fluid (CSF)), bandpass filtering (0.001 Hz, 0.1 Hz), spatial normalization with the diffeomorphic anatomical registration through an exponentiated lie algebra (DARTEL) [Ashburner, 2007] and smoothing with Gaussian isotropic kernel (6 mm of full-width-at-half-maximum). The normalization procedure was facilitated by the use of a study-specific mid-template created with DARTEL. The template was created from the average of T1 images from our patients and healthy controls [Di Perri et al., 2013, 2016; Peelle et al., 2012] to potentially decrease the likelihood of misclassification and normalization errors occurring during the voxel-based morphometry process.

### Co-Activation Patterns Construction

After preprocessing, the dataset was reduced to a spatio-temporal point process [Liu and Duyn, 2013] by selecting time points in the seed region at which the signal is higher than one standard deviation (SD) [Liu and Duyn, 2013]. In this work we used a cube ( $6 \times 6 \times 6 \text{ mm}^3$ ) centered at the posterior cingulate cortex (i.e., PCC, [0, 53, 26] in MNI coordinates, identical to Liu and Duyn [2013]). The PCC was chosen as the seed to study default mode network (DMN) variability in disorders of consciousness, as the PCC is widely known as a central node in the DMN [Laureys et al., 2004; Stamatakis et al., 2010]. The CAPs construction can then be summarized in three steps described by Amico et al. [2014]. Briefly, we first, we

collected all the points in the normalized PCC time course where the BOLD signal was above threshold, here fixed to 1 standard deviation (SD) as in Amico et al. [2014]. Second,  $k$ -means ( $k = 8$ , as in Amico et al. [2014] and Liu and Duyn [2013]) clustering was performed on all the time frames which were significantly co-activated with PCC, to extract 8 different spatial PCC-related co-activation patterns. With the purpose of obtaining a robust benchmark baseline against which to track modifications related to different groups, we first ran  $k$ -means clustering over the PCC time frames collected on an independent dataset from the 1000 Functional Connectome Project (FCP, [www.nitrc.org/projects/fcon\\_1000/](http://www.nitrc.org/projects/fcon_1000/)), which includes wakefulness resting-state fMRI collected at multiple sites (247 subjects), as used by Amico et al. [2014] and Liu and Duyn [2013]. Finally, the eight PCC-CAPs centroids obtained earlier were then kept fixed, and spatial clustering on the PCC time frames extracted for each group (i.e., UWS patients and controls), was then performed around these centroids. This procedure allows comparing PCC-CAPs between groups.

At the end of this procedure, we obtained 8 different CAPs (i.e., spatial patterns activated with the PCC) for each subject group.

### Motion Correction

It has recently been shown that even after standard motion correction, residual head movements can still inflate connectivity measures [Power et al., 2012]. To evaluate the extent of these residual motion artifacts in CAPs, for each subject and for each group, we computed the two indices proposed by Power et al. [2012, 2015], that is, framewise displacement (FD) and DVARS, as in Amico et al. [2014]. FD is a scalar quantity that expresses instantaneous head motion, while DVARS measures how much the intensity of a brain image changes in comparison to the previous time-point [Power et al., 2012, 2015]. Second, we defined frames as “motion corrupted” (“ArtFrames” in Supporting Information, Fig. S1) when FD and DVARS values were both above 0.5 mm for FD and 0.5% bold for DVARS, as suggested in the same paper [Power et al., 2012]. For each group (controls and UWS), we then checked if there were motion corrupted time frames in our CAPs, the percentage of these frames over the whole sample, and whether motion corrupted frames were somehow involved in the CAPs pattern by recomputing the CAPs with and without the motion corrupted frames. Additionally, the signal of each voxel was demeaned and normalized by its temporal SD. The percentage of motion corrupted time frames was 4% for the healthy controls and 10% for the UWS population. However, there was no significant difference between CAPs computed with or without artifact removal (Supporting Information, Fig. S1).

### Statistical Analysis

All statistical analyses were carried out using SPM8. Individual time frames were entered into a second-level analysis, corresponding to a random-effects model in which subjects are considered random variables. These second-level analyses consisted of analyses of variance (repeated measures analysis of variance) with the two clinical conditions as factors: (UWS and controls). The error covariance was not assumed to be independent between regressors; therefore, a correction for nonsphericity was applied. We used one-sided  $T$ -contrasts, as implemented in Statistical Parametric Mapping software, to test for significant effects in all our analyses. After model estimation, a first  $T$ -contrast searched for areas co-activated with the PCC in UWS and healthy controls (contrast +1 for each CAP). The same was done to search for areas deactivated with the PCC (contrast -1 for each CAP). These maps were used as inclusive masks for the intergroup  $t$ -test analyses (i.e.,  $\text{UWS} < \text{controls}$  and  $\text{UWS} > \text{controls}$ ) to effectively calculate the intersection between the positive/negative correlations and the intergroup differences and to constrain within-network or between-network regions. For comparison, the same analyses were carried out using conventional seed-based functional connectivity maps, as previously described [Amico et al., 2014]. Results were considered significant at  $P < 0.05$ , corrected for multiple comparisons with false discovery rate (FDR) [Genovese et al., 2002] at voxel level, as in Boveroux et al. [2010].

To test the temporal occurrences of each CAP, we evaluated the corresponding occurrence as the number of time frames associated to a CAP, divided by the total number of functional frames collected. This gave us a measure of the frequency of the PCC-related functional fluctuations across groups. We then used a double-sided  $t$  test to statistically compare the two different population means for each of the 8 extracted CAPs.

We used a double-sided  $t$  test to statistically compare the two different population means for the total time frames collected.

## RESULTS

### Patients

From December 2009 to December 2015, a number of 76 patients diagnosed as UWS underwent an MRI scan. Following the exclusion criteria (see Flow Chart 1 in Supporting Information), the analysis focused on a convenience sample of 17 UWS patients: (8 males, mean age 43 years SD 15, mean disease duration 29 months SD 27, 8 TBI). All patients underwent structural MRI and resting-state functional MRI scanning. Supporting Information, Table S1 summarizes the patients' clinical and demographic characteristics. A total of 17 age-gender-matched healthy volunteers (8 males, mean age:  $41 \pm 15$  years) were included.



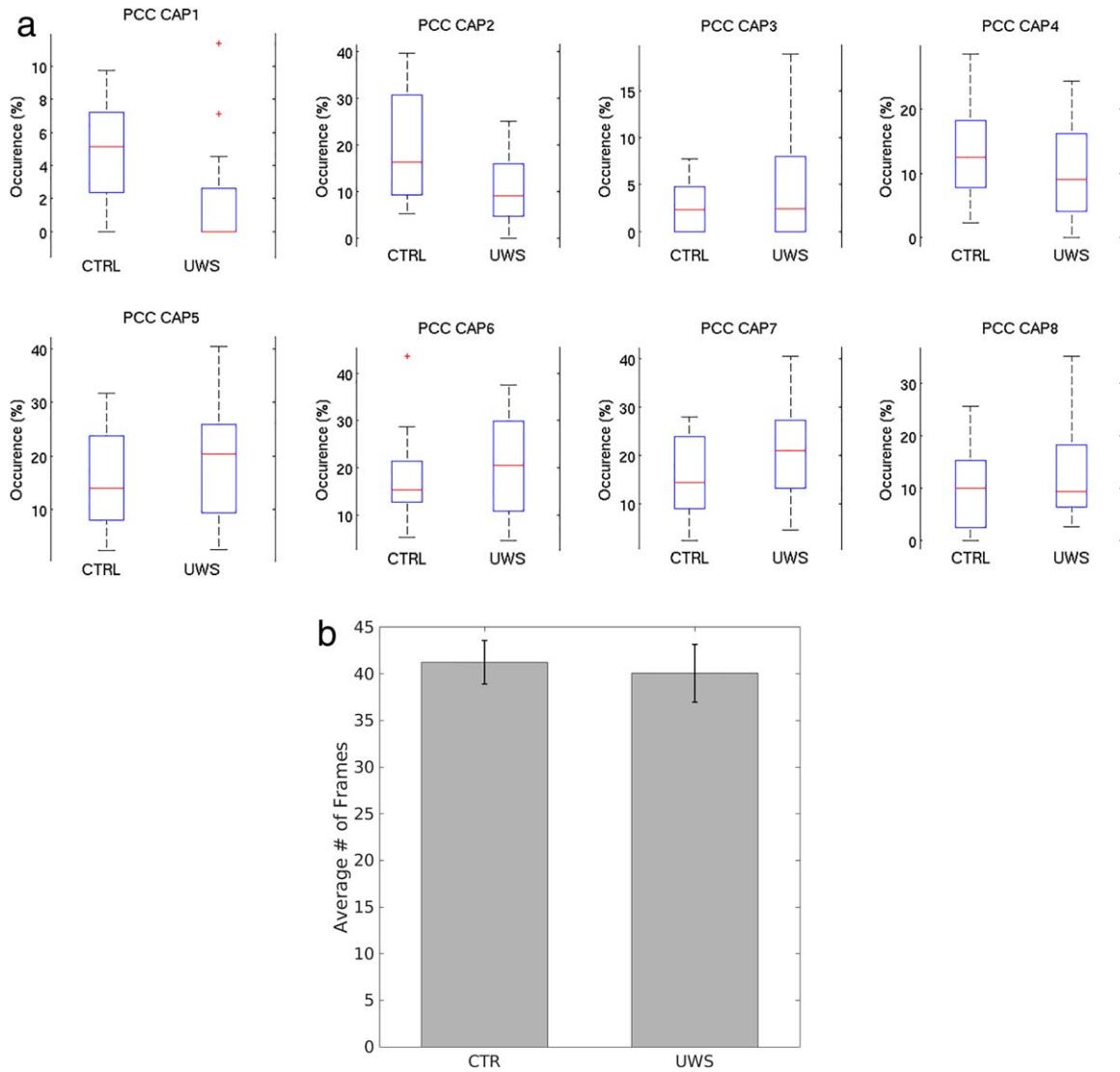


**Figure 1.**

Boxplots show differences in the occurrence of the two populations (i.e., controls and UWS) per each of the 8 CAPs (a). The tops and bottoms of each “box” are the 25th and 75th percentiles of the samples, respectively. The line in the middle of each box is the sample median. The whiskers are drawn from the ends of the interquartile ranges to the furthest observations

within the whisker length (the adjacent values). Red crosses indicate outliers. Note that only CAP 1 and CAP 2 show a significant difference in occurrence across the two groups (a). Bars show the total number of frames in patients and controls (b). CTRL = controls; UWS = unresponsive wakefulness syndrome; PCC = posterior cingulate cortex.

### CAPs: Occurrence

The comparison of the occurrence of CAPs (i.e., co-activation patterns at each time-frame) in the different groups showed a significant difference between groups in CAPs 1 and 2, which are known to be more similar to the DMN structure ( $P < 0.001$ , effect size 2.88 and 2.82, respectively) with higher occurrence in controls as compared to patients (Fig. 1a). No significant differences between the

two groups were observed in the occurrence of CAPs 3, 4, 5, 6, 7, and 8 (Fig. 1a).

### Total Number of Frames

No differences were observed between the total number of time-frames in patients and controls (682 in patients and 701 in controls,  $P = 0.2$ ) (Fig. 1b), suggesting that

BOLD fluctuations are similar in patients and controls. Examples of the signal time course are displayed in Supporting Information, Figure S2.

## CAPS: Spatial Maps

### DMN within-network connectivity

**Controls and patients.** In both controls and patients, the decomposition of the signal into CAPS shows additional and more in depth spatial information than the conventional seed-based approach, with the first CAPS resembling more the DMN spatial maps and the last CAPS resembling sensory networks such as the auditory, visual, and sensory-motor, as previously shown [Amico et al., 2014].

In controls, the decomposition into CAPS shows also the interaction between DMN and regions involving the external awareness network such as insula (CAPs 1 and 6).

The core of the PCC-CAPS seems to be preserved in both conscious controls and unconscious patients, in particular the PCC/precuneus and the temporo-parietal junctions (Fig. 2), confirming what shown in other states of unconsciousness such as propofol-induced unconscious states [Amico et al., 2014] and suggesting that consciousness is not strictly related to connectivity within the DMN.

What seems mostly impaired in patients is the correlation between PCC and hippocampi (seed, CAP1, CAP4, CAP5, CAP6, and CAP8), mesioprefrontal cortex/ACC (seed, CAP1, CAP2, CAP3, CAP4, CAP5, CAP7, and CAP8), and thalami (CAP4, CAP5, CAP6, and CAP8) (Fig. 2, yellow/orange). In contrast, patients mostly show a preserved correlation between the PCC and primary sensory areas such as the auditory network (CAP6), visual network (CAP7), and somatosensory network (CAP8) (Fig. 2, yellow/orange). These results, in line with previous literature, suggest that associative areas such as ACC, PCC, and also hippocampi and thalamus, rather than the primary sensory areas are important for consciousness [Laureys et al., 2004].

**Patients versus controls.** When comparing UWS patients to controls, we find 3 different patterns.

- i. Decreased within-network positive correlations in patients compared to controls (Fig. 3, red). By using a conventional seed-based approach, decreased positive correlations in patients compared to controls are noted in the ACC/mesioprefrontal cortex, precuneus, mesiotemporal, and temporal poles (Fig. 3, red). However, when employing CAPs, additional decreased within-network positive correlations in the lateral right temporal cortex (CAP 2), right intraparietal cortex (CAPs 2, 4, 5, and 6), left insula (CAP 6), cuneus (CAP 7), and left postcentral gyrus (CAP 8) are also observed (Fig. 3, red).
- ii. Pathological increases of within-network positive correlations in patients compared to controls (Fig. 3, yellow). These increases are not observed using the conventional approach, but they are only observed in CAPs. In particular, in UWS, higher within-network positive correlations are observed in the hypothalamus (CAP 2), cuneus (CAP 5), and right insula (CAP 6) (Fig. 3, yellow).
- iii. Pathological emergence of within-network negative correlations in UWS compared to controls (Fig. 3, blue). Using the conventional approach, we observe in UWS increased within-network negative correlations with the PCC in the hippocampi (Fig. 3, blue). CAPs show a more detailed pattern with additional increased within-network negative correlations with PCC in the mesioprefrontal cortex (CAPs 2 and 7), the mesial occipital cortex (CAP 4), and the temporal cortex (CAP 7) (Fig. 3, blue). In simple words, some correlation observed in controls flip signal from positive into negative in unconscious patients, reflecting a change in the dynamic interactions between brain regions in patients, which may have a specific role in sustaining unconscious states.

### DMN between-network connectivity

**Controls and patients.** With respect to between-network connectivity, in controls and patients, the decomposition of the signal into CAPS shows additional and more in-depth spatial information than the conventional seed-based approach. In controls, the conventional seed-based approach shows negative correlations with the PCC in the so-called external awareness network involving the supplementary motor area, the insulae, and lateral frontal and parietal regions [Fox et al., 2005], but also in the cerebellum and to some extent in the visual occipital regions (Fig. 4, blue). CAPs reveal supplementary negative between-network correlations in the cuneus and visual areas (CAPs 1, 4, and 6), lateral occipital cortex (CAPs 5 and 6), thalami (CAP 2), sensorymotor regions (CAP4), and caudatum nuclei (CAP 8) (Fig. 4, blue). In UWS, using a seed-based approach, only limited negative between-network correlations are observed in the lateral temporo-occipital cortex, cerebellum, and supplementary motor area (Fig. 4, green). By investigating the dynamic of the signal using CAPs, additionally between-network negative correlations are observed in the lateral frontal cortex (CAPs 2 and 7), insulae (CAP 2, 4, and 5), sensory-motor areas (CAP 4), cuneus/visual regions (CAP 6), and lateral parietal cortex (CAP 2, 4, and 7) (Fig. 4, green). Here we see a similar pattern as observed in positive within-network correlations, that is, we overall see primary sensory regions such as primary additive (CAP 5), visual (CAP 6), and somatosensory regions (CAP 4) but also cerebellum (CAP 6 and 8) that are mostly preserved in patients, while the lateral

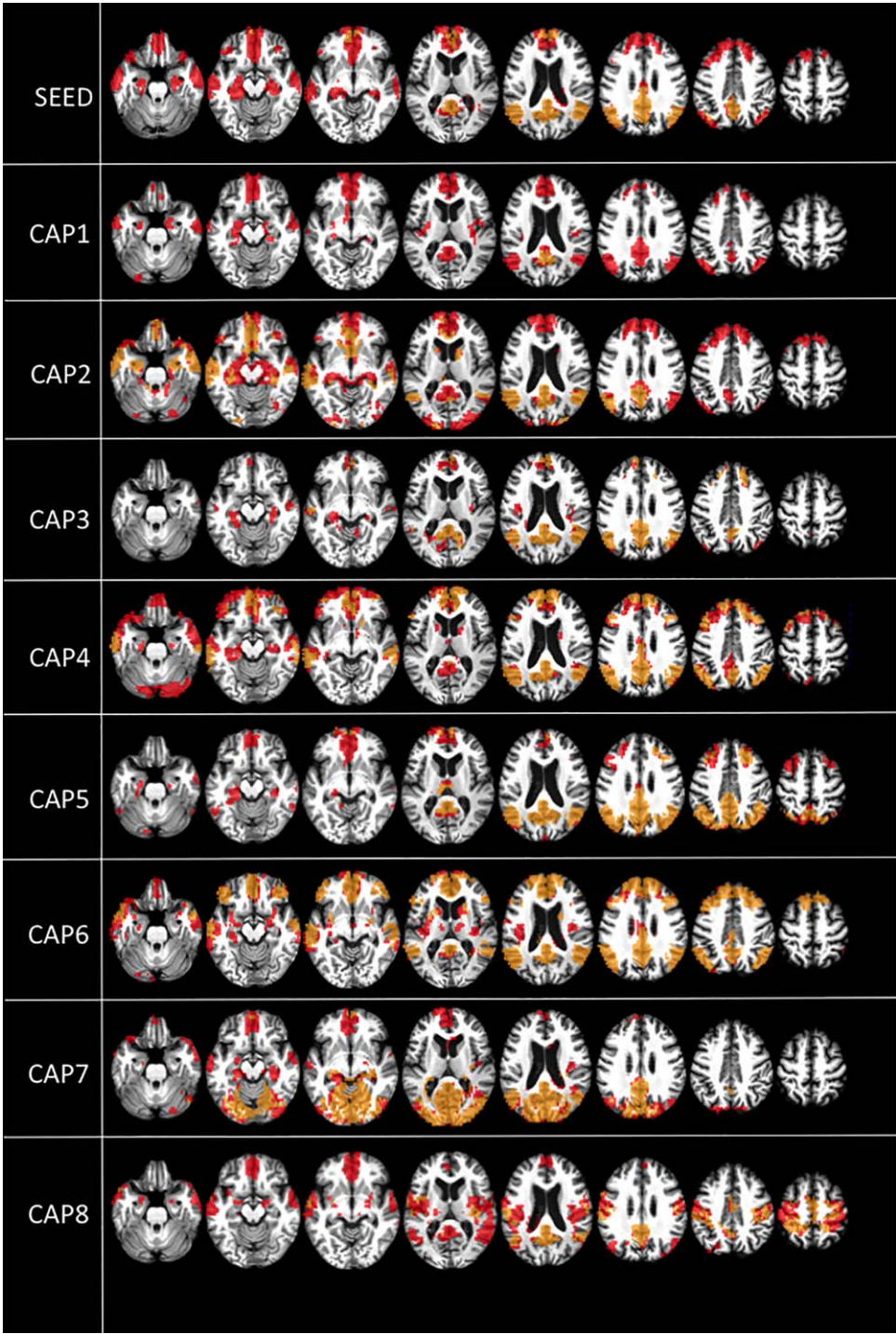


**Figure 2.**

Default mode network (DMN) within-network positive correlations. Positive correlations within the DMN ( $t$  contrast) in healthy controls (red) and unresponsive patients (yellow/orange). Results are shown at  $P < 0.05$  false discovery rate (FDR) corrected. Upper row shows PCC seed-voxel correlation maps. Images are displayed on a T13D study template. CAP = co-activation pattern.



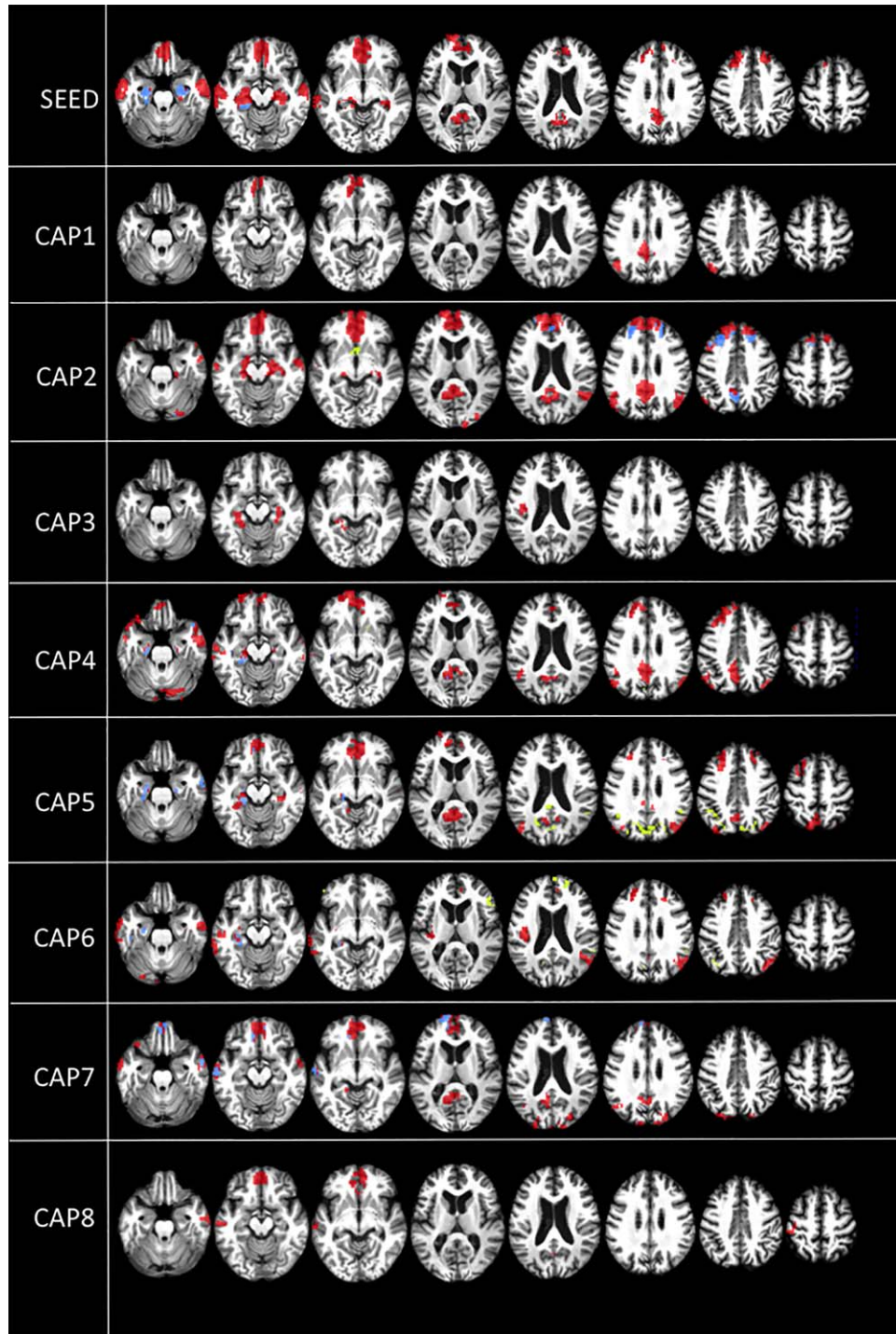


**Figure 3.**

Inter-subject differences in DMN within-network correlations. Within-network positive correlations ( $t$  contrast) in patients < controls (red) and patients > controls (yellow), and emergence of within-network negative correlations in patients compared to

controls (blue). Results are shown at  $P < 0.05$  false discovery rate (FDR) corrected. Upper row shows PCC seed-voxel correlation maps. Images are displayed on a T13D study-template. CAP = co-activation pattern.



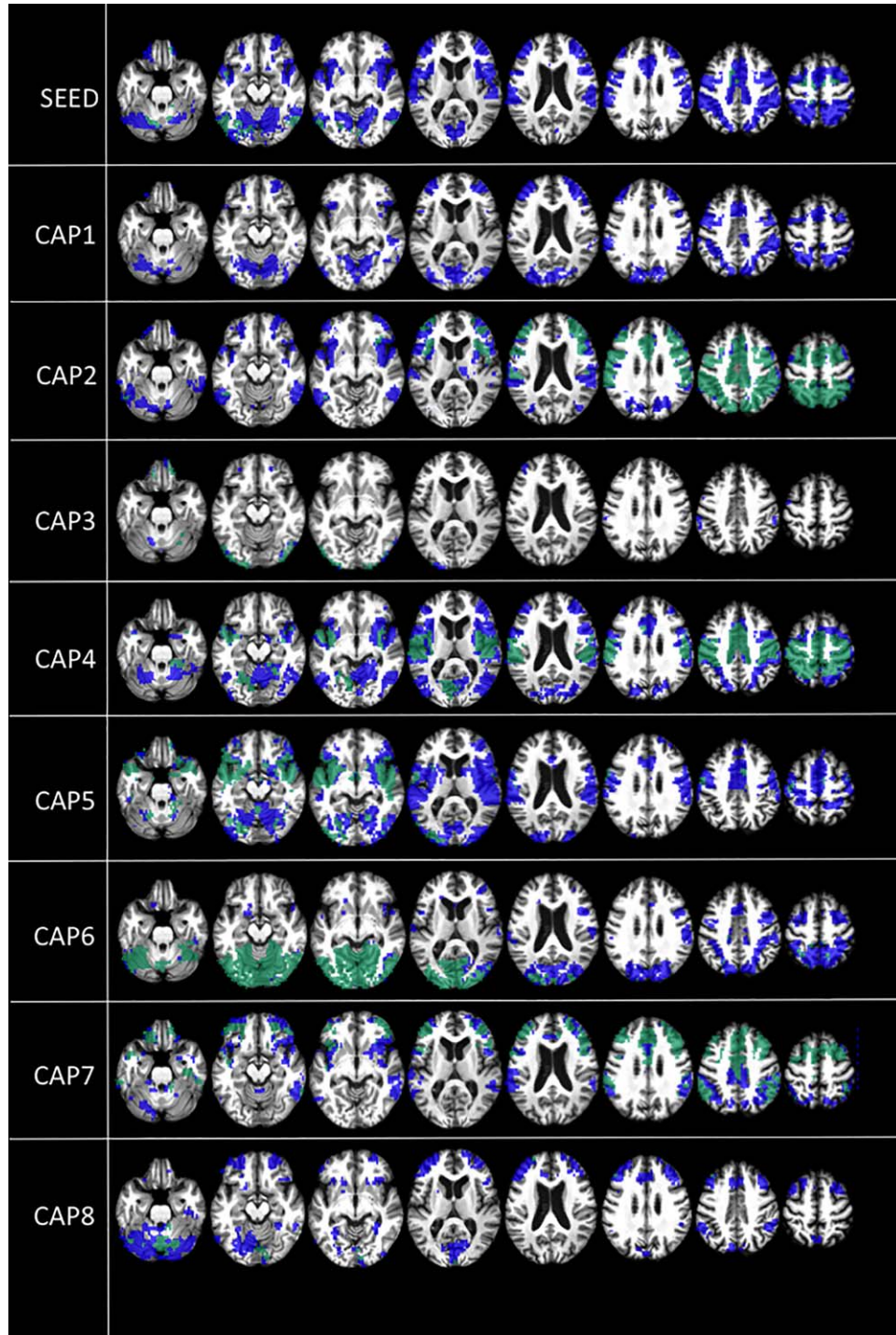


**Figure 4.**

Default mode network (DMN) between-network negative correlations. Between-network negative correlations ( $t$  contrast) in controls (blue) and unresponsive patients (green). Results are shown at  $P < 0.05$  false discovery rate (FDR) corrected. Upper row shows PCC seed-voxel correlation maps. Images are displayed on a T13D study template. CAP = co-activation pattern.

frontoparietal regions seem more inconstantly preserved (Fig. 4, green). This could however be related to the fact that these latter negative correlations are more often represented in the CAPS.

**Patients versus controls.** When directly comparing patients to controls, we find three main between-network connectivity patterns:

- i. Decreased between-network negative correlations in patients compared to controls (Fig. 5, blue). This decreased negative connectivity is noted in the insulae, in the lateral frontoparietal regions, but also in the supplementary motor area when using the standard seed-based approach. When decomposing the signal into CAPS, the connectivity patterns appear more granular and therefore further decreased negative correlations are observed in the cerebellum (CAPs 2, 4, 6, and 7), orbitofrontal cortex (CAP 2), caudatae (CAP 5), and cuneus (CAPs 1, 2, and 6) (Fig. 5, blue).
- ii. Pathological increased between-network negative connectivity in patients compared to controls. This pattern is only observed when investigating the dynamic of the signal with CAPS, in particular increased negative connectivity is observed between PCC and intraparietal sulci and supplementary motor area (CAP2) and inferior left temporal cortex (CAP6) (Fig. 5, green). That might suggest that preserved between-network negative correlations are not per se a sign of consciousness, but also their dynamics play a role. When the balance is lost and negative-correlations appear in specific time points where they are not supposed to, this pattern may relate to impaired consciousness as well.
- iii. Emergence of pathological between-network positive correlations with the PCC in patients compared to controls. These pathological positive correlations involve to some extent the right insula, right frontoparietal cortex, and left temporal cortex (Fig. 5, purple). CAPs display more information by revealing additional between-network positive correlations in the temporo-insular regions and right thalamus (CAP 2), lateral frontal cortex (CAPs 4, 5, and 6), and cuneus (CAPs 4 and 6) (Fig. 5, purple). This represents a pathological between-network dynamic interaction balance which from negative becomes positive and supposedly plays a role in consciousness impairment [Di Perri et al., 2016].

Note that although the concept of correlation is normally Pearson correlation, here for simplicity, we keep using it for the relations between regions as established by each of the 8 CAPs scalar maps. A simplified summary of the within-network and between-network spatial connectivity patterns observed in patients and controls is displayed in Supporting Information, Figure S3.

## DISCUSSION

In previous work, co-activation patterns (CAPs) approach, based on the clustering of instantaneous PCC-related spatial maps (i.e., decomposing in time by spatially overlapping functional networks), has shown to provide more fine-grained DMN related connectivity information in healthy controls [Liu and Duyn, 2013]. We here extend the application of this approach to severely brain-injured unconscious patients, and we further investigated the DMN between-network interactions, CAPs occurrence and total number of frames.

With respect to CAPS occurrence, we found a decreased occurrence of DMN-like CAPs (CAPs 1 and 2) in patients as compared to controls. Such findings confirm a large amount of literature showing that the gravity of DMN connectivity disruption is increasing with the degree of consciousness impairment [Di Perri et al., 2013; Vanhau-denhuysen et al., 2010] further suggest that a heterogeneous spatial reconfiguration is taking place in brain injured unresponsive patients following DMN disruption.

However, we did not find intergroup differences in the total number of frames, suggesting that patients with disorders of consciousness show similar fluctuations of the BOLD signal as controls. Besides providing new insight into the rich dynamic organization of resting state in disorders of consciousness, such findings are in line with recent literature which reports variability in functional connectivity patterns over time, in both anesthetized monkeys and healthy controls [Hutchison et al., 2013]. This suggests that BOLD fluctuation might represent, at least in part, a more intrinsic feature of the signal irrespective of conscious cognitive processing [Hutchison et al., 2013].

When looking at spatial maps, with respect to the DMN within-network connectivity, the conventional seed-based approach shows positive correlations within the DMN, that is, areas involving the mesioprefrontal cortex, the precuneus, temporo-parietal junctions, and hippocampi [Raichle, 2011]. When decomposing the signal into CAPs, our results in healthy controls are in line with previous findings using the same methodology [Amico et al., 2014; Liu and Duyn, 2013]. The first positive CAPs are spatially more similar to the DMN, whereas the last ones resemble the visual and somatosensory networks. The present findings corroborate previous research showing that spatial grouping is still a meaningful representation of resting-state activity, even if the sustained activity of different regions is temporally overlapping [Karahanoğlu and Van De Ville, 2015]. Here, by temporally decomposing the BOLD signal into positive CAPs, we also identified a few patterns where the posterior cingulate cortex (PCC) shows positive co-activations with regions belonging to the external awareness network (e.g., the insula). This is in line with previous work supporting the dynamic nature of the BOLD signal. Using CAPs to functionally decompose the fMRI resting state into spatially and temporally overlapping building blocks, evidence of different interactions of

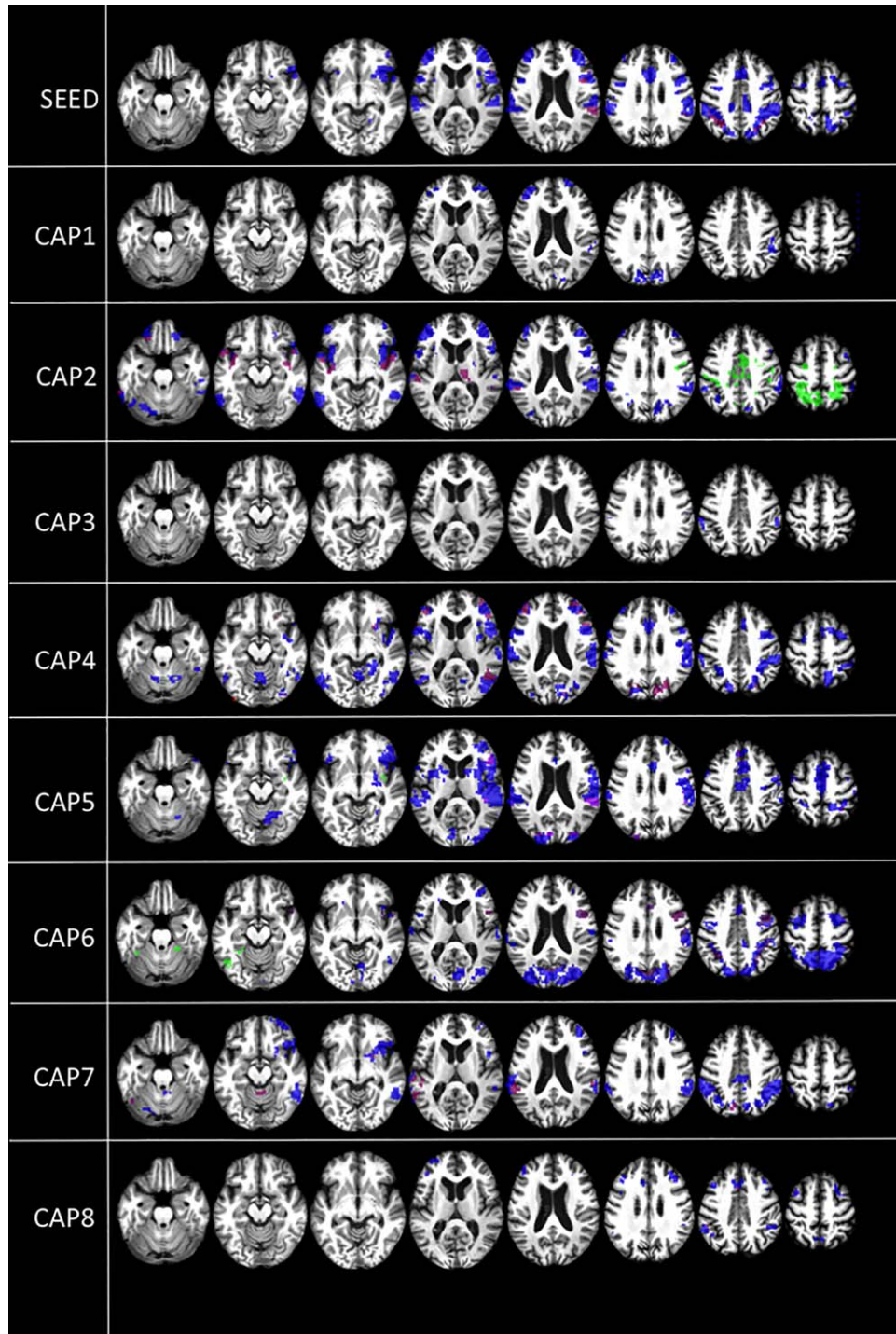


**Figure 5.**

Inter-subject differences in DMN between-network correlations. Between-network negative correlations ( $t$  contrast), where patients < controls (blue), patients > controls (green), and emergence of between-network positive correlations in patients compared to controls (purple). Results are shown at  $P < 0.05$  false discovery rate (FDR) corrected. Upper row shows PCC seed-voxel correlation maps.



the DMN-like CAPs with the external awareness network has previously been found [Karahanoglu and Van De Ville, 2015], suggesting that to some degree, positive correlations between these two networks might not necessarily arise from pathology, and that an altered dynamic balance might indeed generate pathology.

Our findings regarding within-network positive connectivity in patients are similar to those found in Amico et al. [2014]. We here find that unconscious patients mostly show connectivity impairment in the hippocampi, mesio-prefrontal cortex/ACC, and thalamus. On the contrary, connectivity seems preserved in primary sensory areas such as auditory, visual, and somatosensory, suggesting that primary sensory areas do not yield a prominent role in consciousness state rather than associative mesiofrontal DMN regions and thalamus [Laureys, 2005]. However, the fact that in healthy controls and in UWS patients, the core of PCC-CAPS seems to be preserved suggests that positive DMN within-network connectivity is only partially related to consciousness, being a component of it presumably related to intrinsic brain structure [Di Perri et al., 2016; Vincent et al., 2007]. A more complex connectivity reorganization beyond within-network positive connectivity, as here investigated and following discussed, might better shed light on the connectivity processes sustaining unconscious states.

In UWS patients compared to healthy controls, we mainly observed decreased within-network positive correlations, both using the conventional seed-based approach and more thoroughly decomposing the signal into CAPs. This is consistent with a large amount of literature showing a severe disruption of the DMN connectivity in patients with disorders of consciousness [Di Perri et al., 2013, 2016; Vanhaudenhuyse et al., 2010]. However, after decomposing the signal into CAPs, we also observed increased within-network positive activations in patients compared to controls. That suggests that DMN within-positive connectivity is not per se a sign of consciousness, but its dynamics as well play a role. These “pathological” increased activations, not detectable using the standard seed-based approach, mostly involved structures belonging to the limbic system such as the hypothalamus and insula. Such results corroborate previous findings [Di Perri et al., 2013] which suggest that the observed hyperconnectivity might either indicate ancestral and more resistant connections between DMN and limbic structures as a result of the decreased DMN projections in UWS patients or either imply the emergence of possibly dysfunctional self-reinforcing connectivity loops [Di Perri et al., 2013].

Along with decreased and increased within-network positive correlations, patients showed the emergence of “pathological” connectivity patterns, being not observed in controls, such as within-network negative correlations. Indeed, in controls the regions within the DMN show positive correlations, whereas in patients, there is an inversion of the signal, with some regions within the DMN showing

negative correlations with the PCC. This pattern, representing a breakdown of the dynamic connectivity interactions within the DMN which switch from a positive to a negative sign, is better evaluated with CAPs, which show therefore a higher sensitivity.

The aforementioned “pathological” within-network negative correlations appeared to extensively involve the hippocampal-PCC circuit. Hippocampi and PCC, integral nodes of the DMN [Wang et al., 2010], are known to be involved in the encoding and retrieval of information phases and therefore play a crucial role in subserving episodic memory process [Viard et al., 2010; Wang et al., 2010]. Impaired connectivity between these regions have shown to serve as a predictor of memory decline related to early Alzheimer’s disease [Kim et al., 2013]. With regards to consciousness, these pathological negative correlations may represent a specific marker of the disruption of large-scale connections that characterizes patients with UWS. Further studies are warranted to gain a better insight into the role of PCC-hippocampus interactions in conscious awareness, which suggest an alternative anatomical substrate of consciousness to the frontoparietal network [Koch et al., 2016].

In some CAPs, we further observed “pathological” within-network negative co-activations between mesio-prefrontal cortex and PCC, confirming a large amount of literature suggesting that communication (or information transfer) between the different cortical midline regions within the cingulate gyrus has a role in cognitive functions necessary for consciousness [Vanhaudenhuyse et al., 2010].

In general, the above results regarding DMN connectivity suggest that decrease in DMN within-network positive connectivity is only an aspect related to unconsciousness in severely brain-injured patients. Other connectivity patterns, some of them only or better visible investigating the network dynamic interactions seem to be equally involved in sustaining unconsciousness. Among them there are pathological increases of positive within-network correlations, emergence of negative within-network correlations and, as we will now discuss, breakdown of the between-network connectivity balance.

With respect to the DMN between-network connectivity, in healthy controls, the DMN showed negative correlations with regions involved in the external awareness network in accordance with previous literature showing an intrinsic negative correlation in the absence of overt task performances between the two networks [Di Perri et al., 2016; Fox et al., 2005]. These between-network negative correlations (i.e., anticorrelations) have been shown to possibly reflect an effective capacity to switch between an extrospectively oriented and an introspectively oriented behavior [Fransson, 2005], which might be indicative of subjective phenomena and therefore conscious awareness [Demertzi et al., 2013]. Indeed, our past research showed on one hand a correlation between “external awareness” (everything we perceive through our senses) and activity in the



external awareness network, and on the other hand between “internal awareness” (self-related mentation or mind-wandering) and activity in the DMN [Vanhaudenhuyse et al., 2011]. The present findings support previous studies, which report a rich interplay between internal and external modes that accounts for the support of conscious behavior [Leech et al., 2011].

In UWS patients compared to controls, we mainly observed decreased between-network negative correlations, both using the conventional seed-based approach and more thoroughly decomposing the signal into CAPs. This is congruent with previous studies showing the importance of these negative correlations in the emergence of cognitive functions necessary for consciousness [Di Perri et al., 2016]. Moreover, after decomposing the signal into CAPs, we also observed increased between-network negative activations in patients compared to controls. In particular, we found higher negative correlations between the PCC and both the posterior associative parietal cortex and primary sensorimotor regions. This is in line with previous studies indicating the posterior cingulate/precuneus as a key component of the internal awareness network, namely the DMN, and a critical hub for sensory integration necessary for consciousness [Magioncalda et al., 2015; Toussaint et al., 2014; Vanhaudenhuyse et al., 2010; Washington and VanMeter, 2015]. That further suggests that between-network negative connectivity is not per se a sign of consciousness, but its dynamic should also be taken into account. We could speculate that the increased negative correlations between PCC and sensory regions in unresponsive patients may somehow reflect impaired integration of sensory information necessary for conscious awareness.

Along with decreased and increased between-network negative correlations, patients showed the emergence of “pathological” connectivity patterns never observed in controls, that is, the emergence of “pathological” between-network positive correlations, that is, positive correlations between the DMN and the external awareness network. This represents a pathological dynamic interaction between networks, which from negative becomes positive and supposedly play an important role in consciousness impairment. These findings further support previous studies showing the emergence of so-called “pathological hyperconnectivity” in altered states of consciousness [Di Perri et al., 2013]. Specifically, we recently found “pathological” positive correlations between the DMN and the external awareness network in patients with disorders of consciousness, whereas negative between-network correlations were preserved only in healthy controls and partially in patients who had recovered from disorders of consciousness, suggesting that consciousness relies on a specific topological and temporal balance [Di Perri et al., 2016]. Similarly, our results are convergent with reported altered functional hyperconnectivity found in transient unresponsive wakefulness, such as in epilepsy [Blumenfeld, 2012] and anesthetically induced unconsciousness [Guldenmund et al., 2013]. We should however

keep in mind that, although mechanisms underlining the persistence of resting-state activity at higher frequencies are not yet ascertained, positive correlations between DMN and external awareness network have also been observed at higher frequencies bands [Chen and Glover, 2015]. Future studies investigating resting state at higher frequencies in patients and controls are therefore warranted to shed further light on the connectivity patterns sustaining consciousness.

In conclusion, taken together these results suggest that impaired consciousness is not related to BOLD fluctuations per se, neither to a mere decrease of DMN within-network connectivity as previously thought. Different spatial connectivity patterns involving the breakdown of a dynamic balance within and between networks are equally involved in consciousness impairment. These patterns can therefore be better investigated studying the dynamic interactions by decomposing the signal into different CAPs, which reveal at a more fine-grained level the heterogeneous connectivity spatial reconfigurations following decreased DMN within-network connectivity in impaired consciousness patients and might suggest alternative anatomical substrates of consciousness. For example, the DMN within-network hippocampi-PCC circuit might be a marker of consciousness worth to be better investigated in future studies.

The additional spatiotemporal information yielded by this approach provides new insights on the connectivity patterns sustaining disorders of consciousness and in a future perspective can have clinical applications, for example, by being used in a classifier for diagnostic and prognostic purposes.

## CONFLICT OF INTEREST

The authors state that they have no conflict of interest with the content of this article.

## REFERENCES

- Allen EA, Damaraju E, Plis SM, Erhardt EB, Eichele T, Calhoun VD (2014): Tracking whole-brain connectivity dynamics in the resting state. *Cereb Cortex* (New York, N.Y.: 1991) 24:663–676.
- Amico E, Gomez F, Di Perri C, Vanhaudenhuyse A, Lesenfants D, Boveroux P, Bonhomme V, Brichant JF, Marinazzo D, Laureys S (2014): Posterior cingulate cortex-related co-activation patterns: A resting state fMRI study in propofol-induced loss of consciousness. *PLoS One* 9:e100012.
- Ashburner J (2007): A fast diffeomorphic image registration algorithm. *NeuroImage* 38:95–113.
- Blumenfeld H (2012): Impaired consciousness in epilepsy. *Lancet Neurol* 11:814–826.
- Boveroux P, Vanhaudenhuyse A, Bruno MA, Noirhomme Q, Lauwick S, Luxen A, Degueldre C, Plenevaux A, Schnakers C, Phillips C, Brichant JF, Bonhomme V, Maquet P, Greicius MD, Laureys S, Boly M (2010): Breakdown of within- and between-network resting state functional magnetic resonance imaging connectivity during propofol-induced loss of consciousness. *Anesthesiology* 113:1038–1053.

- Chang C, Glover GH (2010): Time-frequency dynamics of resting-state brain connectivity measured with fMRI. *NeuroImage* 50:81–98.
- Chen JE, Glover GH (2015): BOLD fractional contribution to resting-state functional connectivity above 0.1 Hz. *NeuroImage* 107:207–218.
- Damoiseaux JS, Rombouts SA, Barkhof F, Scheltens P, Stam CJ, Smith SM, Beckmann CF (2006): Consistent resting-state networks across healthy subjects. *Proc Natl Acad Sci USA* 103: 13848–13853.
- de Pasquale F, Della Penna S, Snyder AZ, Lewis C, Mantini D, Marzetti L, Belardinelli P, Ciancetta L, Pizzella V, Romani GL, Corbetta M (2010): Temporal dynamics of spontaneous MEG activity in brain networks. *Proc Natl Acad Sci USA* 107: 6040–6045.
- Demertzi A, Vanhaudenhuyse A, Bredart S, Heine L, di Perri C, Laureys S (2013): Looking for the self in pathological unconsciousness. *Front Hum Neurosci* 7:538.
- Di Perri C, Bahri MA, Amico E, Thibaut A, Heine L, Antonopoulos G, Charland-Verville V, Wannez S, Gomez F, Hustinx R, Tshibanda L, Demertzi A, Soddu A, Laureys S (2016): Neural correlates of consciousness in patients who have emerged from a minimally conscious state: A cross-sectional multimodal imaging study. *Lancet Neurol*.
- Di Perri C, Bastianello S, Bartsch AJ, Pistarini C, Maggioni G, Magrassi L, Imberti R, Pichiecchio A, Vitali P, Laureys S, Di Salle F (2013): Limbic hyperconnectivity in the vegetative state. *Neurology* 81:1417–1424.
- Di Perri C, Stender J, Laureys S, Gosseries O (2014): Functional neuroanatomy of disorders of consciousness. *Epilepsy Behav* 30:28–32.
- Fox MD, Snyder AZ, Vincent JL, Corbetta M, Van Essen DC, Raichle ME (2005): The human brain is intrinsically organized into dynamic, anticorrelated functional networks. *Proc Natl Acad Sci USA* 102:9673–9678.
- Fransson P (2005): Spontaneous low-frequency BOLD signal fluctuations: An fMRI investigation of the resting-state default mode of brain function hypothesis. *Hum Brain Mapp* 26:15–29.
- Genovese CR, Lazar NA, Nichols T (2002): Thresholding of statistical maps in functional neuroimaging using the false discovery rate. *NeuroImage* 15:870–878.
- Giacino JT, Fins JJ, Laureys S, Schiff ND (2014): Disorders of consciousness after acquired brain injury: The state of the science. *Nat Rev Neurol* 10:99–114.
- Giacino JT, Kalmar K, Whyte J (2004): The JFK Coma Recovery Scale-Revised: Measurement characteristics and diagnostic utility. *Arch Phys Med Rehabil* 85:2020–2029.
- Guldenmund P, Demertzi A, Boveroux P, Boly M, Vanhaudenhuyse A, Bruno MA, Gosseries O, Noirhomme Q, Brichant JF, Bonhomme V, Laureys S, Soddu A (2013): Thalamus, brainstem and salience network connectivity changes during propofol-induced sedation and unconsciousness. *Brain Connect* 3:273–285.
- Hindriks R, Adhikari MH, Murayama Y, Ganzetti M, Mantini D, Logothetis NK, Deco G (2016): Can sliding-window correlations reveal dynamic functional connectivity in resting-state fMRI? *NeuroImage* 127:242–256.
- Hutchison RM, Womelsdorf T, Allen EA, Bandettini PA, Calhoun VD, Corbetta M, Della Penna S, Duyn JH, Glover GH, Gonzalez-Castillo J, Handwerker DA, Keilholz S, Kiviniemi V, Leopold DA, de Pasquale F, Sporns O, Walter M, Chang C (2013): Dynamic functional connectivity: Promise, issues, and interpretations. *NeuroImage* 80:360–378.
- Kang J, Wang L, Yan C, Wang J, Liang X, He Y (2011): Characterizing dynamic functional connectivity in the resting brain using variable parameter regression and Kalman filtering approaches. *NeuroImage* 56:1222–1234.
- Karahanoglu FI, Van De Ville D (2015): Transient brain activity disentangles fMRI resting-state dynamics in terms of spatially and temporally overlapping networks. *Nat Commun* 6:7751.
- Kim J, Kim YH, Lee JH (2013): Hippocampus-precuneus functional connectivity as an early sign of Alzheimer's disease: A preliminary study using structural and functional magnetic resonance imaging data. *Brain Res* 1495:18–29.
- Kiviniemi V, Vire T, Remes J, Elseoud AA, Starck T, Tervonen O, Nikkinen J (2011): A sliding time-window ICA reveals spatial variability of the default mode network in time. *Brain Connect* 1:339–347.
- Koch C, Massimini M, Boly M, Tononi G (2016): Neural correlates of consciousness: Progress and problems. *Nat Rev Neurosci* 17:307–321.
- Laumann TO, Snyder AZ, Mitra A, Gordon EM, Gratton C, Adeyemo B, Gilmore AW, Nelson SM, Berg JJ, Greene DJ, McCarthy JE, Tagliazucchi E, Laufs H, Schlaggar BL, Dosenbach NU, Petersen SE (2016): On the Stability of BOLD fMRI correlations. *Cereb cortex* (New York, N.Y.: 1991).
- Laureys S (2005): The neural correlate of (un)awareness: Lessons from the vegetative state. *Trends Cogn Sci* 9:556–559.
- Laureys S, Celesia GG, Cohadon F, Lavrijsen J, Leon-Carrion J, Sannita WG, Szabon L, Schmutzhard E, von Wild KR, Zeman A, Dolce G (2010): Unresponsive wakefulness syndrome: A new name for the vegetative state or apallic syndrome. *BMC Med* 8:68.
- Laureys S, Owen AM, Schiff ND (2004): Brain function in coma, vegetative state, and related disorders. *Lancet Neurol* 3:537–546.
- Leech R, Kamourieh S, Beckmann CF, Sharp DJ (2011): Fractionating the default mode network: Distinct contributions of the ventral and dorsal posterior cingulate cortex to cognitive control. *J Neurosci* 31:3217–3224.
- Leonardi N, Van De Ville D (2015): On spurious and real fluctuations of dynamic functional connectivity during rest. *NeuroImage* 104:430–436.
- Lindquist MA, Xu Y, Nebel MB, Caffo BS (2014): Evaluating dynamic bivariate correlations in resting-state fMRI: A comparison study and a new approach. *NeuroImage* 101:531–546.
- Liu X, Chang C, Duyn JH (2013): Decomposition of spontaneous brain activity into distinct fMRI co-activation patterns. *Front Syst Neurosci* 7:101.
- Liu X, Duyn JH (2013): Time-varying functional network information extracted from brief instances of spontaneous brain activity. *Proc Natl Acad Sci USA* 110:4392–4397.
- Magioncalda P, Martino M, Conio B, Escelsior A, Piaggio N, Presta A, Marozzi V, Rocchi G, Anastasio L, Vassallo L, Ferri F, Huang Z, Roccatagliata L, Pardini M, Northoff G, Amore M (2015): Functional connectivity and neuronal variability of resting state activity in bipolar disorder—reduction and decoupling in anterior cortical midline structures. *Hum Brain Mapp* 36:666–682.
- Peelle JE, Cusack R, Henson RN (2012): Adjusting for global effects in voxel-based morphometry: Gray matter decline in normal aging. *NeuroImage* 60:1503–1516.
- Power JD, Barnes KA, Snyder AZ, Schlaggar BL, Petersen SE (2012): Spurious but systematic correlations in functional connectivity MRI networks arise from subject motion. *NeuroImage* 59:2142–2154.
- Power JD, Schlaggar BL, Petersen SE (2015): Recent progress and outstanding issues in motion correction in resting state fMRI. *NeuroImage* 105:536–551.

- Raichle ME (2011): The restless brain. *Brain Connect* 1:3–12.
- Shakil S, Lee CH, Keilholz SD (2016): Evaluation of sliding window correlation performance for characterizing dynamic functional connectivity and brain states. *NeuroImage* 133:111–128.
- Stamatakis EA, Adapa RM, Absalom AR, Menon DK (2010): Changes in resting neural connectivity during propofol sedation. *PLoS One* 5:e14224.
- Tagliazucchi E, Balenzuela P, Fraiman D, Chialvo DR (2012): Criticality in large-scale brain fMRI dynamics unveiled by a novel point process analysis. *Front Physiol* 3:15.
- Toussaint PJ, Maiz S, Coynel D, Doyon J, Messe A, de Souza LC, Sarazin M, Perlberg V, Habert MO, Benali H (2014): Characteristics of the default mode functional connectivity in normal ageing and Alzheimer’s disease using resting state fMRI with a combined approach of entropy-based and graph theoretical measurements. *NeuroImage* 101:778–786.
- Vanhaudenhuyse A, Demertzi A, Schabus M, Noirhomme Q, Bredart S, Boly M, Phillips C, Soddu A, Luxen A, Moonen G, Laureys S (2011): Two distinct neuronal networks mediate the awareness of environment and of self. *J Cogn Neurosci* 23:570–578.
- Vanhaudenhuyse A, Noirhomme Q, Tshibanda LJ, Bruno MA, Boveroux P, Schnakers C, Soddu A, Perlberg V, Ledoux D, Brichant JF, Moonen G, Maquet P, Greicius MD, Laureys S, Boly M (2010): Default network connectivity reflects the level of consciousness in non-communicative brain-damaged patients. *Brain* 133:161–171.
- Vatansever D, Menon DK, Manktelow AE, Sahakian BJ, Stamatakis EA (2015): Default mode dynamics for global functional integration. *J Neurosci* 35:15254–15262.
- Viard A, Lebreton K, Chetelat G, Desgranges B, Landeau B, Young A, D, La Sayette V, Eustache F, Piolino P (2010): Patterns of hippocampal-neocortical interactions in the retrieval of episodic autobiographical memories across the entire life-span of aged adults. *Hippocampus* 20:153–165.
- Vincent JL, Patel GH, Fox MD, Snyder AZ, Baker JT, Van Essen DC, Zempel JM, Snyder LH, Corbetta M, Raichle ME (2007): Intrinsic functional architecture in the anaesthetized monkey brain. *Nature* 447:83–86.
- Wang L, Laviolette P, O’Keefe K, Putcha D, Bakkour A, Van Dijk KR, Pihlajamaki M, Dickerson BC, Sperling RA (2010): Intrinsic connectivity between the hippocampus and posteromedial cortex predicts memory performance in cognitively intact older individuals. *NeuroImage* 51:910–917.
- Washington SD, VanMeter JW (2015): Anterior-posterior connectivity within the default mode network increases during maturation. *Int J Med Biol Front* 21:207–218.